



High shear stress relates to intraplaque haemorrhage in asymptomatic carotid plaques

Tuenter, A.; Selwaness, M.; Arias Lorza, A.; Schuurbijs, J. C. H.; Speelman, L.; Cibis, M.; van der Lugt, A.; de Bruijne, Marleen; van der Steen, A. F. W.; Franco, O. H.; Vernooij, M. W.; Wentzel, J. J.

Published in:
Atherosclerosis

DOI:
[10.1016/j.atherosclerosis.2016.05.018](https://doi.org/10.1016/j.atherosclerosis.2016.05.018)

Publication date:
2016

Document version
Publisher's PDF, also known as Version of record

Document license:
[CC BY](#)

Citation for published version (APA):
Tuenter, A., Selwaness, M., Arias Lorza, A., Schuurbijs, J. C. H., Speelman, L., Cibis, M., van der Lugt, A., de Bruijne, M., van der Steen, A. F. W., Franco, O. H., Vernooij, M. W., & Wentzel, J. J. (2016). High shear stress relates to intraplaque haemorrhage in asymptomatic carotid plaques. *Atherosclerosis*, 251, 348–354. <https://doi.org/10.1016/j.atherosclerosis.2016.05.018>



High shear stress relates to intraplaque haemorrhage in asymptomatic carotid plaques



A. Tuentjer^{a, b, c, d}, M. Selwaness^{a, c, d}, A. Arias Lorza^e, J.C.H. Schuurbiers^a, L. Speelman^a, M. Cibis^a, A. van der Lugt^d, M. de Bruijne^{e, f}, A.F.W. van der Steen^a, O.H. Franco^c, M.W. Vernooij^{c, d}, J.J. Wentzel^{a, *}

^a Department of Cardiology, Biomedical Engineering, Erasmus MC, Rotterdam, The Netherlands

^b Netherlands Institute for Health Sciences, Rotterdam, The Netherlands

^c Department of Epidemiology, Erasmus MC, Rotterdam, The Netherlands

^d Department of Radiology, Erasmus MC, Rotterdam, The Netherlands

^e Biomedical Imaging Group Rotterdam, Departments of Medical Informatics, Radiology & Nuclear Medicine, Erasmus MC, Rotterdam, The Netherlands

^f Department of Computer Science, University of Copenhagen, Denmark

ARTICLE INFO

Article history:

Received 17 November 2015

Received in revised form

29 April 2016

Accepted 7 May 2016

Available online 8 May 2016

Keywords:

Carotid artery

Atherosclerosis

Shear stress

Vulnerable plaque

MRI

ABSTRACT

Background and aims: Carotid artery plaques with vulnerable plaque components are related to a higher risk of cerebrovascular accidents. It is unknown which factors drive vulnerable plaque development. Shear stress, the frictional force of blood at the vessel wall, is known to influence plaque formation. We evaluated the association between shear stress and plaque components (intraplaque haemorrhage (IPH), lipid rich necrotic core (LRNC) and/or calcifications) in relatively small carotid artery plaques in asymptomatic persons.

Methods: Participants (n = 74) from the population-based Rotterdam Study, all with carotid atherosclerosis assessed on ultrasound, underwent carotid MRI. Multiple MRI sequences were used to evaluate the presence of IPH, LRNC and/or calcifications in plaques in the carotid arteries. Images were automatically segmented for lumen and outer wall to obtain a 3D reconstruction of the carotid bifurcation. These reconstructions were used to calculate minimum, mean and maximum shear stresses by applying computational fluid dynamics with subject-specific inflow conditions. Associations between shear stress measures and plaque composition were studied using generalized estimating equations analysis, adjusting for age, sex and carotid wall thickness.

Results: The study group consisted of 93 atherosclerotic carotid arteries of 74 participants. In plaques with higher maximum shear stresses, IPH was more often present (OR per unit increase in maximum shear stress (log transformed) = 12.14; $p = 0.001$). Higher maximum shear stress was also significantly associated with the presence of calcifications (OR = 4.28; $p = 0.015$).

Conclusions: Higher maximum shear stress is associated with intraplaque haemorrhage and calcifications.

© 2016 The Authors. Published by Elsevier Ireland Ltd. This is an open access article under the CC BY license (<http://creativecommons.org/licenses/by/4.0/>).

1. Introduction

Atherosclerosis in the carotid arteries represents an important cause of ischemic stroke [1]. The composition of atherosclerotic plaques is an important predictor for plaque rupture and

subsequent thromboembolic events [2]. Plaques that contain a large lipid rich necrotic core (LRNC), intraplaque haemorrhage (IPH), inflammation and/or are covered by a thin fibrous cap are considered the most vulnerable to rupture [3–5]. Conversely, the presence of calcifications has been associated with a more stable plaque phenotype [6,7].

The development of a vulnerable plaque is a complex process which is still not completely understood. Initially, plaque size or lumen obstruction were thought of as the most important determinants of plaque vulnerability, but these explain variability in

* Corresponding author. Head Biomechanics Laboratory, Biomedical Engineering Department of Cardiology, Room Ee2338, Erasmus MC, P.O. Box 2040, 3000 CA, Rotterdam, The Netherlands.

E-mail address: j.wentzel@erasmusmc.nl (J.J. Wentzel).

plaque rupture only to a limited extent [8]. One hypothesis is that plaque vulnerability may be influenced by hemodynamic forces occurring in blood vessels [9]. It is known that plaques develop at distinct locations in the arterial system, for instance, the inner curve, close to side branches and in the bulbs of the carotid artery [10–12]. At these locations, the shear stress, the drag force of the blood at the vessel wall, is mainly low and/or oscillatory. There is ample evidence that low shear stress is involved in plaque initiation and progression through various molecular mechanisms that influence endothelial cell morphology and function [8,13–15]. In animal studies and small case studies an association between shear stress and plaque composition was observed [16,17]. Though low shear stress may induce plaque initiation, it has been hypothesized that plaque destabilization can be caused by high shear stress on the plaque [9]. Yet, to date little is known on the association between shear stress and plaque composition in human carotid arteries. Particularly asymptomatic plaques have little been studied in this respect, whereas understanding of plaque progression in the preclinical stage could provide useful targets for prevention.

Magnetic resonance imaging (MRI) has emerged as a non-invasive imaging modality that enables accurate identification of the main components of the atherosclerotic plaque [18]. Furthermore, it allows quantification of the blood flow through the artery, which can be used to derive the shear stress on the vessel wall and plaque. The objective of this study was to evaluate the association between shear stress and the different plaque components (IPH, LRNC and calcifications) in carotid arteries by combining MRI and computational fluid dynamics (CFD) in asymptomatic participants with carotid atherosclerosis of a population-based cohort.

2. Materials and methods

2.1. Study population

This study was embedded within the Rotterdam Study, a prospective cohort study conducted in the Ommoord district of Rotterdam. The Rotterdam Study targets to study causes and consequences of age-related diseases, including atherosclerosis, in a general middle-aged and elderly population (>45 years). The baseline visit started between 1990 and 1993 and participants were invited every 3–4 years for a range of examinations. Starting from October 2007 all participants were invited for an ultrasound of the carotid arteries. If the ultrasound showed arterial wall thickening of more than 2.5 mm in one of the carotid arteries, participants were invited for an MRI of both carotid arteries. Participants were excluded when there were contraindications for MRI, an endarterectomy was performed or when the image quality was poor [19]. For the present study, the MRI scans of the first 104 participants were chosen, as computational fluid dynamics is a very labour intensive measurement.

Fig. 1 shows a flow chart explaining the reasons for exclusion of a number of carotid arteries in the final data analysis. We started with the flow calculations of 208 carotid arteries. In 82 carotid arteries flow calculations could not be completed, mainly because of problems in segmentation (carotid artery arms were cut off too short, arms were connected or images were unavailable) or unreliable flow measurements. If the flow ratio between the internal and the common carotid artery was outside the normal range of 40–70% [20], the flow measurements were deemed unreliable and thus reason to exclude the carotid. Subsequently, for 9 carotid arteries shear stress could not be generated due to post-processing problems and of the remaining 117 carotid arteries, only 99 had a wall thickness of more than 1.5 mm, the threshold for plaque presence. For 93 carotid arteries plaque composition information was available and for those 93 carotid arteries of 74 participants the

final analyses were done.

The Rotterdam Study has been approved by the medical ethics committee according to the Population Study Act Rotterdam Study, executed by the Ministry of Health Welfare and Sports of the Netherlands. All participants gave written informed consent in order to participate in the study [21].

2.2. MRI of carotid arteries

Carotid plaque MR imaging was performed with a 1.5 T scanner (GE Signa Excite II; Healthcare, Milwaukee, WI, USA) using a bilateral phased-array surface coil (Machnet, Eelde, the Netherlands) with a slice thickness of 1.2 mm. The total scanning time was about 30 minutes, and a standard scanning protocol was present, that included multiple MR sequences [21]: 4 2D axial sequences (a) PDw Fast Spin Echo (FSE) Black-blood (BB) sequence with fat suppression; (b) PDw-FSE-BB sequence with an increased in-plane resolution (0.51 mm); (c) a PDw-EPI sequence; (d) T2w-EPI sequence, and two 3D sequences (I) 3DT1w- GRE sequence parallel to the common carotid artery, and (II) 3D phased-contrast MRI (3D PC MRI). Sequence parameters have been described in detail elsewhere and are also available as an online supplement [19]. The 3D PC MRI sequence allows to determine the local velocities in 3 directions in each cross section at the in plane resolution. These velocity measurements are the average over the cardiac cycle and thus the average flow over the cardiac cycle can be determined. Using the PDw-FSE images, percentage of luminal stenosis was calculated according to the North American Symptomatic Carotid Endarterectomy Trial (NASCET) criteria [22].

2.3. Determining plaque composition

Plaque composition was scored when the image quality on all MRI sequences was sufficient (image quality was scored ≥ 3 on a five-point scale). Two trained observers scored carotid artery plaques for the presence of three plaque components: lipid rich necrotic core, intraplaque haemorrhage and calcifications as described before [19]. IPH was defined as the presence of a hyperintense region of the atherosclerotic plaque on 3D-T1w-GRE. LRNC presence was defined as a hypointense region, not classified as intraplaque haemorrhage or calcification, in the plaque on PDw-FSE or PDw-EPI and T2w-EPI images, or a region of relative signal intensity drop in the T2w-EPI images compared with the PDw-EPI images. Calcification was defined as the presence of a hypointense region in the plaque on all sequences. Inter-observer agreement was good for all measurements with Cohen's Kappa ranging from 0.86 (IPH and LRNC) to 0.94 (calcification) [19]. Fig. 2 shows the different plaque components as visible on MRI.

2.4. Shear stress calculations

Shear stress was calculated using an in-house written framework, 'the BioStress tool'. The BioStress tool is a matlab network that streamlines the various steps that need to be taken to calculate shear stress using computational fluid dynamics (CFD). As an input for this tool the 3D lumen surface was segmented using an in-house developed validated automatic segmentation tool, detecting lumen and outer wall surface in the black-blood MRI and PDw-EPI images [23]. The segmentations were obtained from all available MRI cross sections covering the largest possible distance along the vessel within the margins of acceptable image quality. The viscosity was modeled according to the Carreau model. Subsequently, the BioStress tool was used for: I) smoothing of the 3D lumen surface and outer wall to generate a volume mesh and adding extensions (3 times the diameter) to the common, internal and external carotid

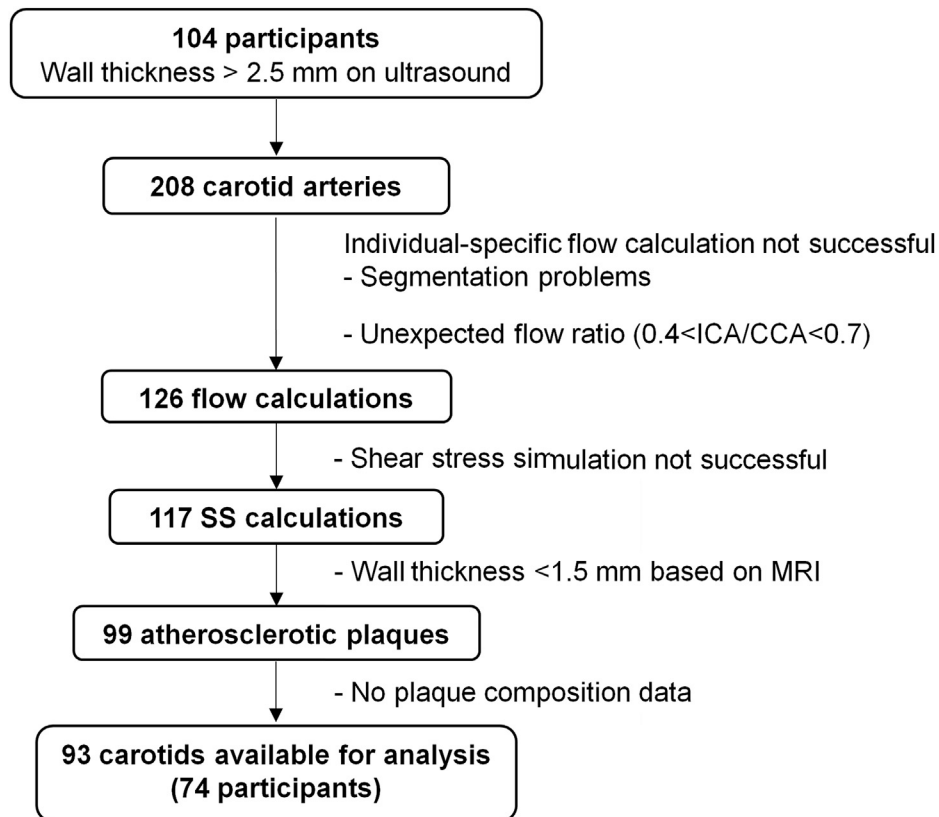


Fig. 1. Flow diagram of participants included and excluded from the study. The reasons for exclusion of participants are shown on the right side.

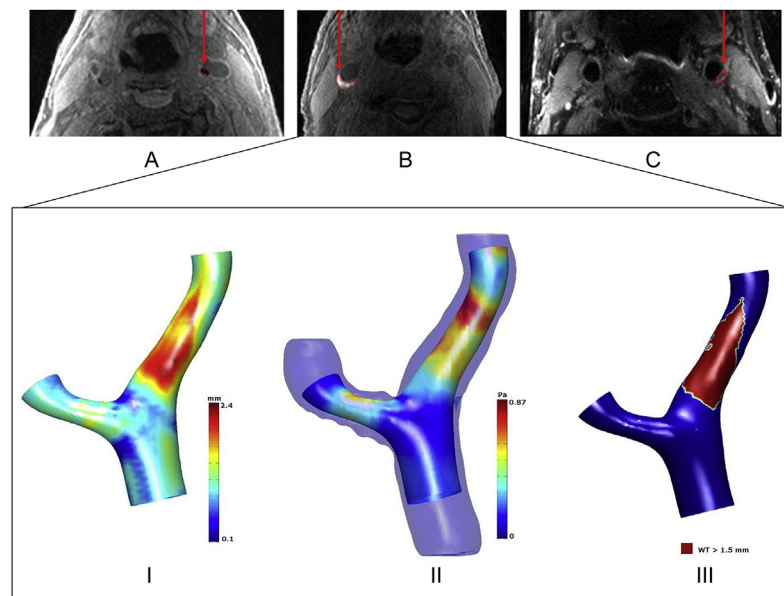


Fig. 2. MRI images depicting the different plaque components. Panels show calcification (A), intraplaque haemorrhage (B) and lipid-rich necrotic core (C). Note that a combination of sequences is used to rate the presence of each component, as described extensively in van den Bouwhuisen et al. [19], but for illustrative purposes, only a single image is shown here (in A and B: T1-weighted gradient-echo image; in B: proton-density weighted echo planar imaging). For the carotid artery plaque depicted in (B) containing IPH, the 3D geometry with wall thickness (I), shear stress (II) and plaque location (III) are shown.

arteries to minimize the influence of the entrance inflow conditions; II) selecting the inflow and outflow conditions; III) creating a batch file with all measured person specific inflow conditions in the common carotid artery (CCA) as input for the CFD simulations. CCA

flow was based on the 3D PC-MRI measurement of velocities in a plane perpendicular to the central axis of the common carotid artery, yielding a single time-averaged flow as input for the stationary CFD calculations. Since flow measurements using PC-MRI suffer

from inaccuracies related to partial voluming, in particular at the stationary vessel wall, ghosting and noise, the flows in the first 5 consecutive frames were averaged. The flow was calculated by multiplying the average velocity in the cross section with the cross sectional area; IV) initiating the shear stress calculation using computational fluid dynamics by execution of the finite element software package FIDAP. For the stationary CFD calculations the following boundary conditions were applied: at the CCA inlet a parabolic inflow profile with person specific flow, the outflow of the ECA was set at 40% of the CCA flow, while the ICA was left stress free [20]. Using a stress free outflow condition in the vessel under study, CFD can be performed without any assumption on the outflow velocity profile. The walls were considered rigid and a no-slip condition was applied. The CFD calculations took 1–5 h for each carotid artery. Since the MRI coils that were used for imaging of the carotid arteries deliver the most optimal image quality over a length of 25 mm and images were acquired with the bifurcation as reference in the center, our analysis of shear stress, wall thickness and plaque composition was performed 12 mm proximal to the bifurcation and 13 mm distal from the bifurcation. By combining the shear stress calculations with the wall thickness measurements (Fig. 2), plaque areas with a wall thickness > 1.5 mm were detected and at those locations minimum (SS_{\min}), mean (SS_{mean}) and maximum shear stress (SS_{\max}) were determined. By calculating SS_{\min} , SS_{mean} and SS_{\max} in the entire plaque area of each carotid artery, these three absolute values in each carotid artery were used for statistical analysis.

3. Statistical analyses

Shear stresses were not normally distributed and were therefore log-transformed before running the statistical analyses. Associations between shear stress across the plaque and plaque composition were studied using logistic regression analysis. A general linear model was used with plaque composition (plaque component present yes/no) as the outcome parameter and shear stress (minimum, mean and maximum) as the determinant. This analysis was repeated with as determinant shear stress quartiles. To correct for within-participant correlations between both carotid arteries, we used generalized estimating equation analysis. Associations were analysed in two models: model 1. Adjusted for age and sex; 2. Adjusted for age, sex and carotid maximum wall thickness. Additional adjustment for maximum wall thickness was performed since an increase in wall thickness potentially influences lumen geometry and thus the local shear stress.

All analyses were performed using IBM SPSS statistics version 22. Data are expressed as mean \pm standard deviation for quantitative variables and percentages for discrete variables. Associations between shear stress and plaque composition are presented as odds ratios with 95% confidence intervals (CI).

4. Results

The baseline characteristics of the 74 asymptomatic participants are shown in Table 1. Mean age of the study population was 75 ± 11 years, 50% of the participants were women and 73% of the participants had hypertension. Calcifications, LRNC and IPH were present in 72%, 31% and 22% of the carotid arteries, respectively. In Table 2 the results of the logistic regression analysis are presented relating shear stress to plaque composition. Adjustments were made in 2 models: 1) adjusted for age and sex; 2) adjusted for age, sex and maximum wall thickness. A higher SS_{\max} was associated with presence of IPH (odds ratio (OR) 12.14 (95% CI 3.21–45.94, $p = 0.001$ (model 2)). None of the shear stress measures was significantly associated with the presence of a LRNC. Maximum

Table 1

Baseline characteristics of the study population.

	Participants included in study (n = 74)
Age (y)	74.8 (± 10.5)
Women	37 (50%)
BMI (kg/m^2)	26.7 (2.9)
Total cholesterol (mmol/L)	5.3 (0.9)
HDL (mmol/L)	1.42 (0.4)
Systolic blood pressure (mmHg)	143.93 (21.1)
Diastolic blood pressure (mmHg)	78.71 (10.5)
Hypertension ^a	54 (73%)
Current smokers	13 (17.6%)
Past smokers	39 (52.7%)
Diabetes Mellitus	12 (16.2%)
Flow (ml/s)	4.44 (1.24)
Lumen stenosis (%) ^b	11 (12) ^c
Mean shear stress in plaque area (Pa)	1.26 (1.12)

Values are means \pm SD for continuous variables and percentages for dichotomous variables.

^a Hypertension: systolic blood pressure ≥ 140 or diastolic blood pressure ≥ 90 or BP lowering medication with indication hypertension.

^b Percentage of luminal stenosis was calculated according to the North American Symptomatic Carotid Endarterectomy Trial (NASCET) criteria [22].

^c Not for all persons lumen stenosis was present, n = 72.

shear stress was related to the presence of calcifications with an OR 4.28 (95% CI 1.33–13.82, $p = 0.015$ (model 2)).

Fig. 3 illustrates these results by showing the prevalence of the different plaque components across quartiles of SS_{\min} , SS_{mean} and SS_{\max} . Higher maximum shear stress showed a significant trend across the quartiles for IPH ($p\text{-trend} = 0.013$) and calcifications ($p\text{-trend} = 0.011$). Minimum/mean shear stress quartiles were not significantly associated with presence of LRNC, IPH or calcifications.

5. Discussion

In 74 persons with asymptomatic carotid atherosclerosis, who were sampled from a population-based setting, we evaluated the association between shear stress and carotid plaque composition. We found an association between higher maximum shear stresses and the presence of IPH and calcifications, but not LRNC. This association was independent from maximum plaque thickness.

We calculated shear stress using computational fluid dynamics (CFD) because of the high accuracy of this method [24]. Although shear stress calculation based on CFD is a time consuming method (up to 5 h per carotid artery), we were able to do so for 93 carotid arteries, which is a large dataset compared to similar studies [25–28]. The large number of studied vessels increases generalizability to other asymptomatic persons with atherosclerosis.

For our calculations, we used person-specific flow rates instead of standard flows, which allowed us to calculate absolute shear stress instead of relative shear stress and increases person specificity.

We found that higher maximum shear stress relates to presence of IPH. The pathophysiology of IPH is not completely clear, but the main existing hypothesis is that it develops by rupture of the vasa vasorum or immature neovessels [29]. IPH was shown to be associated with luminal stenosis, which can give rise to an increase in shear stress [29]. This might imply outward remodelling is not so effective if IPH is causing plaque growth. Hence, a possible explanation of the association between high maximum shear stress and IPH can be found in the effect of IPH on an atherosclerotic plaque, as IPH can accelerate plaque growth and thus lumen narrowing. A potential confounder of this association is wall thickness, considering higher wall thickness is associated with higher shear stress (because of luminal stenosis), but also with more severe plaques, which more often contain IPH. By adjusting for the maximum

Table 2

Odds ratios (95% confidence interval) calculated by generalized estimating equations analysis.

	LRNC	p-value	IPH	p-value	Calcification	p-value
SS_{min}^a						
Model 1	0.82 (0.36–1.86)	0.636	0.49 (0.14–1.76)	0.273	0.96 (0.43–2.14)	0.912
Model 2	0.94 (0.40–2.21)	0.894	0.53 (0.15–1.94)	0.340	1.06 (0.44–2.52)	0.901
SS_{mean}^a						
Model 1	1.32 (0.43–4.04)	0.625	3.10 (0.89–10.77)	0.076	2.55 (0.88–7.28)	0.084
Model 2	1.40 (0.44–4.44)	0.567	3.49 (0.94–12.97)	0.062	2.80 (0.93–8.47)	0.068
SS_{max}^a						
Model 1	1.12 (0.30–4.19)	0.863	12.35 (3.27–46.73)	<0.001	4.46 (1.39–14.31)	0.012
Model 2	1.10 (0.29–4.16)	0.887	12.14 (3.21–45.94)	<0.001	4.28 (1.33–13.82)	0.015

Model 1: adjusted for age, sex.

p < 0.05 is given in bold.

Model 2: model 1 + adjusted for maximum wall thickness.

LRNC = lipid rich necrotic core; IPH = intraplaque haemorrhage; SS_{min} = minimum shear stress; SS_{mean} = mean shear stress; SS_{max} = maximum shear stress.^a Log transformed.

plaque thickness we minimized the confounding effect of wall thickness. The association between high shear stress and IPH is interesting as both parameters are investigated for their involvement in plaque vulnerability, plaque rupture and stroke [30].

Shear stress influences the development of an atherosclerotic plaque by affecting endothelial cell alignment and function [14]. For that reason, it is assumed that in areas with low or oscillatory shear stress lipids can more easily migrate into the vessel wall. We expected to find co-localization of low shear stress areas with plaques containing a lipid rich necrotic core. Yet, this association was not seen in our study. Perhaps the large variation of atherosclerosis stages in this population-based group influenced our results. Low shear stress mainly plays a role in plaque initiation and it seems likely that the association between low shear stress and LRNC may not be present in more developed plaques [15]. It is possible that even in asymptomatic persons shear stress is already higher than average, even though the plaque does not cause severe stenosis at that point.

The association we found between high maximum shear stress and the presence of calcifications can be partly caused by the high prevalence of calcifications in plaques that are more severe. During plaque development, shear stress remains constant for a long period, but when plaque formation causes luminal stenosis, shear stress starts to increase [31]. Luminal stenosis occurs in presence of more developed plaques and possibly the association between presence of calcifications and high maximum shear exists due to this pathophysiology. However, the degrees of stenosis were low in this study population with a mean of 10% (SD 11%) stenosis. Out of 94 carotid arteries, 90 were mildly stenosed (<30% NASCET). Likely because of the low degree of stenosis in this population, shear stress was only weakly associated with luminal stenosis and we decided to adjust for maximum wall thickness only. When adjusting for maximum wall thickness we still found this association, suggesting that there are also other, unknown, factors that influence this relation.

In this study we were able to assess the association between shear stress and the presence of different plaque composites. We did not quantify the size of certain plaque components, because of the inaccuracies in determining these areas. Although areas of IPH can be detected accurately [32], this is a lot more difficult for LRNC. This could be an interesting subject for future studies.

Previous studies on shear stress in the carotid arteries focussed on differences between volunteers and patients and its relationship with wall thickness and plaque growth rather than on plaque composition [33–35]. We are not aware of any other study investigating the relationship between shear stress and carotid plaque composition in a large group of patients/subjects using the combination of computational fluid dynamics and MRI. The only study that described correlations between plaque composition and shear

stress in patients was on a new framework to link carotid endarterectomy to shear stress computed in MRI based 3D reconstructions [36]. In 8 vessels they studied correlations between shear stress and plaque composition and found that IPH was associated with lower shear stress, which is in contrast to our paper. However, this paper was not intended to draw firm conclusion on these relationships based on this small group of samples yet. On top of that no flow measurements were performed and thus this work relies on assumed flow values and no conclusions can be drawn regarding the absolute shear stress values. In animals more often the causal relationship between shear stress and plaque composition was studied after modifying the flow in the carotid artery [37]. These studies showed a clear relationship between low shear stress and features of vulnerable plaque.

In coronary arteries, however, a number of studies were performed on the relationship between plaque composition and shear stress. In contrast to the current study, significant relations were found for lipid rich necrotic core versus shear stress. A study by Esthehardi et al. found an inverse relationship between shear stress and percentage necrotic core for plaques with relatively low plaque burden [38]. In addition, in a more severe diseased group of vessels, Wentzel et al. found that the necrotic core of plaques with a large plaque burden (>40%) was most often exposed to higher shear stress [39]. These two studies differ from the current study in the carotid arteries by its more local shear stress assessment and the use of ultrasound based virtual histology for the assessment of plaque composition. The before described relations might have been missed with the current analysis method or MRI might assess the plaque composition differently.

Additionally, some studies are performed correlating changes in plaque composition based on intravascular ultrasound to shear stress [40,41]. They found a positive association between higher shear stress and increase in necrotic core and calcifications. Interestingly, also at low shear stress regions an increase in necrotic core was observed. Plaque burden and plaque phenotype had incremental value on top of shear stress in predicting an increase in necrotic core area [41]. The main difference between the study of Samady et al. and our study was that our study was performed in asymptomatic arteries while their study was performed in symptomatic arteries. Secondly, they measured shear stress and plaque composition at two time points, making it possible to give insight in the development over time. These data would imply that high shear stress exposure of the plaques with IPH as observed in our study potentially leads to an increase in plaque vulnerability over time.

There are some limitations we need to consider. Unfortunately, the use of individual-specific flows challenges the statistical power of our analyses, as we were not able to calculate flow rates of a number of carotid arteries. This was partly caused by problems in

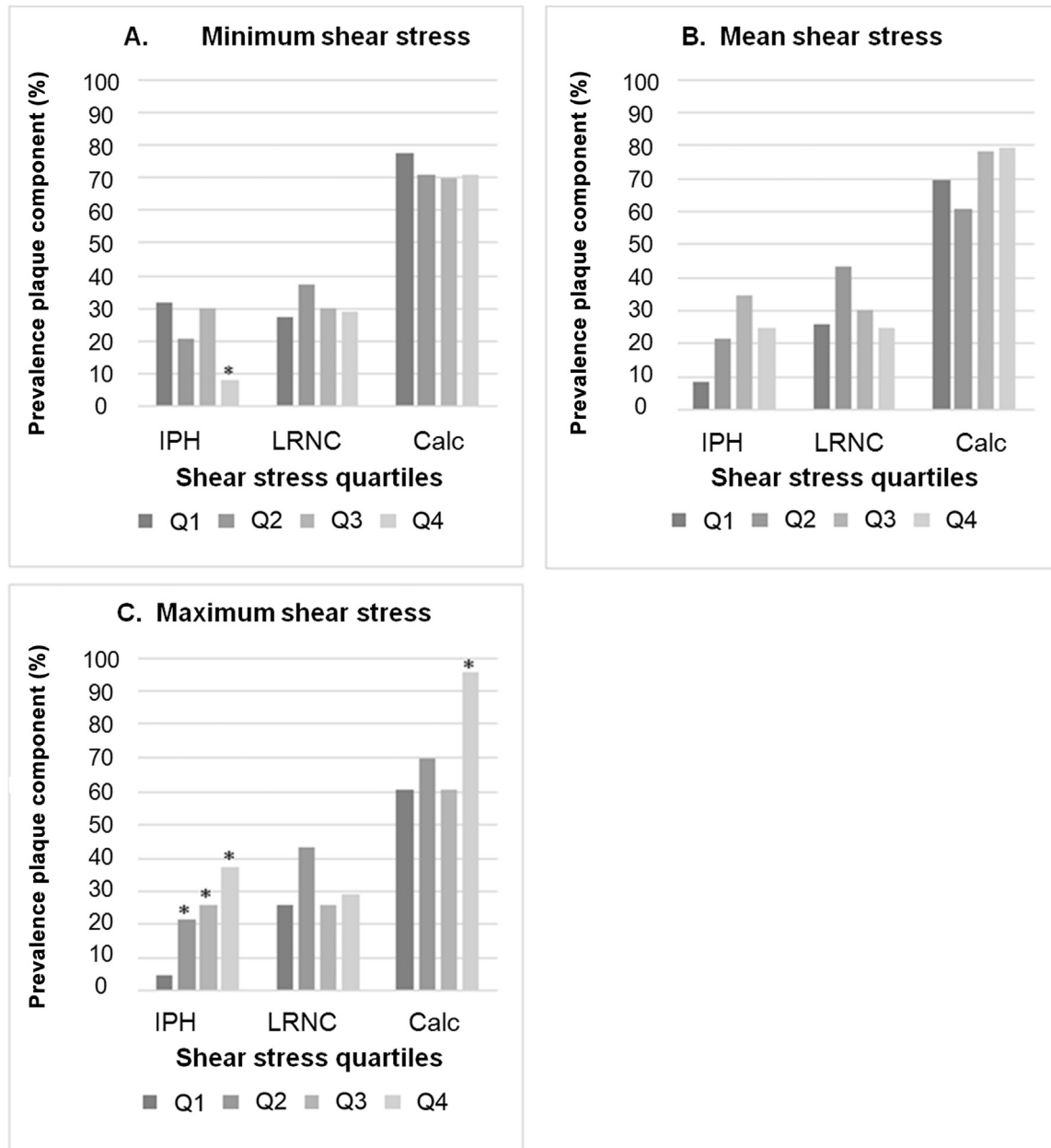


Fig. 3. Prevalence of the different plaque components across quartiles (Q1, Q2, Q3, Q4) of shear stress. Panels show the prevalence of plaque components vs quartiles (Q1, Q2, Q3, Q4) of minimum shear stress (panel A), mean shear stress (panel B), maximum shear stress (panel C). *Significant as compared to lowest shear stress quartiles. *p*-values were calculated using generalized estimating equation analysis, results were adjusted for age, sex and maximum wall thickness. IPH = intraplaque haemorrhage; LRNC = lipid rich necrotic core; Calc = calcification.

the automated segmentation of the carotid bifurcation due to poor image quality. Therefore, it is important to optimize the imaging strategy and segmentation tool for future studies.

The cross-sectional nature of our study limits interpretation of cause and effect in the associations we found. Though we presumed that shear stress induces changes in plaque composition, we cannot rule out the reverse association, i.e. that plaque composition altered the calculated shear stress over the plaque. Only a longitudinal study design, assessing shear stress and plaque composition both at baseline and follow up, will be able to unravel this potential bidirectional association.

When calculating shear stresses by CFD, arterial wall is assumed to be rigid. Considering IPH is softer and weaker than other plaque components [42], it cannot be excluded that this led to an

overestimation of shear stress in plaques containing IPH. However, since the plaque is generally thick in the presence of IPH, this effect is presumably small.

In conclusion, we found that higher maximum shear stress is associated with the presence of calcifications and intraplaque haemorrhage in atherosclerotic carotid plaques of asymptomatic persons. More research is necessary to determine the causality between hemodynamic factors and plaque composition.

Conflict of interest

The authors declared that they do not have anything to disclose regarding conflict of interest with respect to this manuscript.

Financial support

JJW is supported by ERC starters grant, BioCCora 310457 ♥.
AAL is supported by the Technology Foundation (STW, 10813).
MdB is supported by the Netherlands Organisation for Scientific Research (NWO, VIDI 639.022.010).
MC is supported by the Technology Foundation (STW, Carisma, IBISSA, 11629).
MS is supported by the Dutch Heart Foundation (NHS, 2009B044).
LS is supported by the Technology Foundation (STW, 12548).

Appendix A. Supplementary data

Supplementary data related to this article can be found at <http://dx.doi.org/10.1016/j.atherosclerosis.2016.05.018>.

References

- [1] M. Hollander, et al., Carotid plaques increase the risk of stroke and subtypes of cerebral infarction in asymptomatic elderly: the Rotterdam Study, *Circulation* 105 (24) (2002) 2872–2877.
- [2] H.C. Stary, et al., A definition of advanced types of atherosclerotic lesions and a histological classification of atherosclerosis. A report from the committee on vascular lesions of the council on arteriosclerosis, American Heart Association, *Circulation* 92 (5) (1995) 1355–1374.
- [3] H.R. Underhill, et al., Predictors of surface disruption with MR imaging in asymptomatic carotid artery stenosis, *AJNR Am. J. Neuroradiol.* 31 (3) (2010) 487–493.
- [4] A. Gupta, et al., Carotid plaque MRI and stroke risk: a systematic review and meta-analysis, *Stroke* 44 (11) (2013) 3071–3077.
- [5] J.A. Schaer, et al., Terminology for high-risk and vulnerable coronary artery plaques. Report of a meeting on the vulnerable plaque, June 17 and 18, 2003, Santorini, Greece, *Eur. Heart J.* 25 (12) (2004) 1077–1082.
- [6] B. Wu, et al., How does calcification influence plaque vulnerability? Insights from fatigue analysis, *Sci. World J.* 2014 (2014) 417324.
- [7] K.K. Wong, et al., Effect of calcification on the mechanical stability of plaque based on a three-dimensional carotid bifurcation model, *BMC Cardiovasc. Disord.* 12 (2012) 7.
- [8] U. Sadat, et al., Biomechanical structural stresses of atherosclerotic plaques, *Expert Rev. Cardiovasc. Ther.* 8 (10) (2010) 1469–1481.
- [9] H.C. Groen, et al., High shear stress influences plaque vulnerability part of the data presented in this paper were published in *Stroke* 2007;38:2379–2381, *Neth. Heart J.* 16 (7–8) (2008) 280–283.
- [10] C.K. Zarins, et al., Carotid bifurcation atherosclerosis. Quantitative correlation of plaque localization with flow velocity profiles and wall shear stress, *Circ. Res.* 53 (4) (1983) 502–514.
- [11] T. Asakura, et al., Flow patterns and spatial distribution of atherosclerotic lesions in human coronary arteries, *Circ. Res.* 66 (4) (1990) 1045–1066.
- [12] A. Gnasso, et al., In vivo association between low wall shear stress and plaque in subjects with asymmetrical carotid atherosclerosis, *Stroke* 28 (5) (1997) 993–998.
- [13] G. Dai, et al., Distinct endothelial phenotypes evoked by arterial waveforms derived from atherosclerosis-susceptible and -resistant regions of human vasculature, *Proc. Natl. Acad. Sci. U. S. A.* 101 (41) (2004) 14871–14876.
- [14] A.M. Malek, et al., Hemodynamic shear stress and its role in atherosclerosis, *JAMA* 282 (21) (1999) 2035–2042.
- [15] M.A. Gimbrone Jr., et al., Endothelial dysfunction, hemodynamic forces, and atherogenesis, *Ann. N. Y. Acad. Sci.* 902 (2000) 230–239 discussion 9–40.
- [16] Y.S. Chatzizisis, et al., Prediction of the localization of high-risk coronary atherosclerotic plaques on the basis of low endothelial shear stress: an intravascular ultrasound and histopathology natural history study, *Circulation* 117 (8) (2008) 993–1002.
- [17] C. Cheng, et al., Shear stress-induced changes in atherosclerotic plaque composition are modulated by chemokines, *J. Clin. Investig.* 117 (3) (2007) 616–626.
- [18] C. Yuan, et al., In vivo accuracy of multispectral magnetic resonance imaging for identifying lipid-rich necrotic cores and intraplaque hemorrhage in advanced human carotid plaques, *Circulation* 104 (17) (2001) 2051–2056.
- [19] Q.J. van den Bouwhuisen, et al., Determinants of magnetic resonance imaging detected carotid plaque components: the Rotterdam Study, *Eur. Heart J.* 33 (2) (2012) 221–229.
- [20] H.C. Groen, et al., MRI-based quantification of outflow boundary conditions for computational fluid dynamics of stenosed human carotid arteries, *J. Biomech.* 43 (12) (2010) 2332–2338.
- [21] A. Hofman, et al., The Rotterdam Study: 2014 objectives and design update, *Eur. J. Epidemiol.* 28 (11) (2013) 889–926.
- [22] North American Symptomatic Carotid Endarterectomy Trial, Methods, patient characteristics, and progress, *Stroke* 22 (6) (1991) 711–720.
- [23] A. Arias, et al., Carotid artery wall segmentation by coupled surface graph cuts, in: B. Menze, G. Langs, L. Lu, A. Montillo, Z. Tu, A. Criminisi (Eds.), *Medical Computer Vision Recognition Techniques and Applications in Medical Imaging*, Springer, Berlin Heidelberg, 2013, pp. 38–47.
- [24] M. Cibis, et al., Wall shear stress calculations based on 3D cine phase contrast MRI and computational fluid dynamics: a comparison study in healthy carotid arteries, *NMR Biomed.* 27 (7) (2014) 826–834.
- [25] D. Gallo, et al., An insight into the mechanistic role of the common carotid artery on the hemodynamics at the carotid bifurcation, *Ann. Biomed. Eng.* 43 (1) (2015) 68–81.
- [26] S.W. Lee, et al., Geometry of the carotid bifurcation predicts its exposure to disturbed flow, *Stroke* 39 (8) (2008) 2341–2347.
- [27] D. Tang, et al., Image-based modeling for better understanding and assessment of atherosclerotic plaque progression and vulnerability: data, modeling, validation, uncertainty and predictions, *J. Biomech.* 47 (4) (2014) 834–846.
- [28] C. Yang, et al., Impact of flow rates in a cardiac cycle on correlations between advanced human carotid plaque progression and mechanical flow shear stress and plaque wall stress, *Biomed. Eng. Online* 10 (61) (2011) 10–61.
- [29] N. Takaya, et al., Presence of intraplaque hemorrhage stimulates progression of carotid atherosclerotic plaques: a high-resolution magnetic resonance imaging study, *Circulation* 111 (21) (2005) 2768–2775.
- [30] F. Gijzen, et al., Shear stress and advanced atherosclerosis in human coronary arteries, *J. Biomech.* 46 (2) (2013) 240–247.
- [31] J.J. Wentzel, et al., Extension of increased atherosclerotic wall thickness into high shear stress regions is associated with loss of compensatory remodeling, *Circulation* 108 (1) (2003) 17–23.
- [32] H. Tang, et al., Semi-automatic MRI segmentation and volume quantification of intra-plaque hemorrhage, *Int. J. Comput. Assist. Radiol. Surg.* 10 (1) (2015) 67–74.
- [33] M. Cibis, et al., Relation between wall shear stress and carotid artery wall thickening MRI versus CFD, *J. Biomech.* 10 (16) (2016) 30098–30107.
- [34] D. Tang, et al., Correlations between carotid plaque progression and mechanical stresses change sign over time: a patient follow up study using MRI and 3D FSI models, *Biomed. Eng. Online* 12 (2013) 105.
- [35] J.N. Oshinski, et al., Mean-average wall shear stress measurements in the common carotid artery, *J. Cardiovasc. Magn. Reason.* 8 (5) (2006) 717–722.
- [36] G. Canton, et al., A framework for the co-registration of hemodynamic forces and atherosclerotic plaque components, *Physiol. Meas.* 34 (9) (2013) 977–990.
- [37] L.C. Winkel, et al., Animal models of surgically manipulated flow velocities to study shear stress-induced atherosclerosis, *Atherosclerosis* 241 (1) (2015) 100–110.
- [38] P. Eshtehardi, et al., Association of coronary wall shear stress with atherosclerotic plaque burden, composition, and distribution in patients with coronary artery disease, *J. Am. Heart Assoc.* 1 (4) (2012) 24.
- [39] J.J. Wentzel, et al., In vivo assessment of the relationship between shear stress and necrotic core in early and advanced coronary artery disease, *Euro-Intervention* 9 (8) (2013) 989–995.
- [40] H. Samady, et al., Coronary artery wall shear stress is associated with progression and transformation of atherosclerotic plaque and arterial remodeling in patients with coronary artery disease, *Circulation* 124 (7) (2011) 779–788.
- [41] M.T. Corban, et al., Combination of plaque burden, wall shear stress, and plaque phenotype has incremental value for prediction of coronary atherosclerotic plaque progression and vulnerability, *Atherosclerosis* 232 (2) (2014) 271–276.
- [42] Z. Teng, et al., A uni-extension study on the ultimate material strength and extreme extensibility of atherosclerotic tissue in human carotid plaques, *J. Biomech.* 48 (14) (2015) 3859–3867.